Inorganic Chemistry

Article

pubs.acs.org/IC

Luminescence Properties and Energy Transfer of Eu/Mn-Coactivated $Mg_2Al_4Si_5O_{18}$ as a Potential Phosphor for White-Light LEDs

Jian Chen, Yangai Liu,* Minghao Fang, and Zhaohui Huang

School of Materials Science and Technology, China University of Geosciences (Beijing), Beijing 100083, P. R. China

ABSTRACT: A series of blue-to-white emitting $Mg_2Al_4Si_5O_{18}$: Eu^{2+}, Mn^{2+} phosphors were synthesized via high-temperature solid-state method, and their luminescence properties were investigated in detail. Under near-ultraviolet (UV) light excitation of 365 nm, Eu^{2+}-doped $Mg_2Al_4Si_5O_{18}$ exhibits a broad blue emission band peaked at 469 nm, and Mn^{2+}-doped $Mg_2Al_4Si_5O_{18}$ shows a broad orange-red emission band near 600 nm. The energy transfer from Eu^{2+} to Mn^{2+} in $Mg_2Al_4Si_5O_{18}$ host matrix can be found, and the resonant type is demonstrated by a dipole−quadrupole mechanism. The emission hue can be tuned from blue (0.17, 0.17) to bluish green (0.22, 0.29) and finally to white (0.31, 0.33) by properly varying the ratio of Eu^{2+}/Mn^{2+}. The thermal quenching property of the sample was investigated, and the activation energy ΔE was estimated to be 0.30 eV. Additionally, the energy transfer critical distance between Eu^{2+} and Mn^{2+} was calculated. With appropriate tuning of activator content, the $Mg_2Al_4Si_5O_{18}$: Eu^{2+}, Mn^{2+} phosphor may have potential application for UV light-emitting diodes.

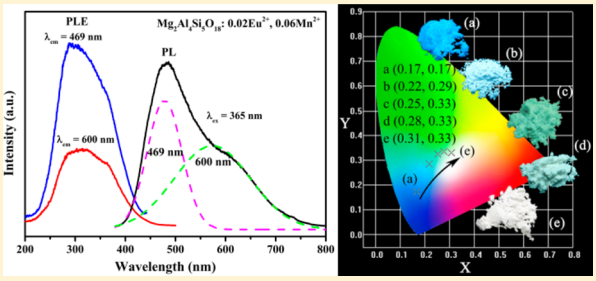

1. INTRODUCTION

It is well-known that white light emitting diodes (*w*-LEDs) have attracted increasing attention to be a next-generation light source owing to their low power consumption, eco-friendliness, and high brightness characteristics in comparison with traditional fluorescent lamps and light source.[1−3] The commercial *w*-LEDs, which are assembled via blue LED chip and yellow-emitting phosphor, have a high efficiency, whereas they have a poor color rendering index because of lacking a red contribution.[4] Additionally, the application of *w*-LEDs based on blue InGaN chip on mass manufacturing scale were restricted due to low color reproducibility. Presently, a near-UV (n-UV) LED (350−420 nm) combined with red, green, and blue (RGB) multiphased phosphors was introduced, which can obtain high color rendering index and suitable correlated color temperature of light. However, in this new class of white LED, the efficiency of blue emission is poor due to the strong reabsorption of red or green emissions from the blue light, and it also has a high cost problem to manufacture such devices.[5] Therefore, many efforts have been made to investigate the single-phased white-emitting phosphors based on the energy transfer mechanism via codoping activator and sensitizer into the same host.[3,6,7]

The Mn^{2+} ions doped into a host lattice show a broad band emission originated from the $^4T_1 \rightarrow {}^6A_1$ transition within the 3d shell in which the electrons are strongly coupled to lattice vibration and influenced by site symmetry and crystal field strength of host.[8] Hence, The emission of Mn^{2+} changes from green (strong crystal field) to red (weak crystal field), which relies on the crystal field strength of host. However, the absorption and emission of Mn^{2+} are weak owing to the forbidden d−d transitions of Mn^{2+}. It is well-known that Eu^{2+} is an efficient sensitizer that transfers energy to Mn^{2+} in numerous hosts.[9−17] Therefore, the energy transfer of $Eu^{2+} \rightarrow Mn^{2+}$ in phosphors has been investigated actively in the recent years. Since the $Eu^{2+} \rightarrow Mn^{2+}$ energy transfer process was first developed in $BaMg_2Si_2O_7$: Eu^{2+}, Mn^{2+},[8] numerous advances have been brought to *w*-LEDs. Up to now, the process of the $Eu^{2+} \rightarrow Mn^{2+}$ energy transfer has been found in many systems and the energy transfer mechanism has been investigated for a long time. Rubio et al.[10] established an ionic radius criterion model to predict paring between two impurity dopant ions in alkali halide host matrix, which could furnish a rational basis to choose suitable impurity dopant ions for developing efficient phosphors. After that, the ionic radius criterion proposed was substantiated by Caldino et al. via $CaCl_2$: Eu^{2+}, Mn^{2+} single crystals.[11,12] Mendez et al.[13] demonstrated the mechanism of energy transfer from Eu^{2+} to Mn^{2+} can be considered that a dipole−quadrupole or exchange (superexchange) interaction mechanism actively exist in the Eu^{2+}−Mn^{2+} cluster formation. Currently, the $Eu^{2+} \rightarrow Mn^{2+}$ energy transfer can be used in many systems as a phosphor for fabrication of a *w*-LEDs, such as $Ba_3MgSi_2O_8$: Eu^{2+},Mn^{2+},[5] $SrZn_2(PO_4)_2$: Eu^{2+},Mn^{2+},[14] $CaAl_2Si_2O_8$: Eu^{2+},Mn^{2+}[15] and $Ca_2MgSi_2O_7$: Eu^{2+},Mn^{2+}.[16] But still few studies focus on the thermal quenching property, which is one of the important properties for phosphors using in *w*-LEDs.

Because of their good material stability, cheap raw materials, and easy preparation, $Mg_2Al_4Si_5O_{18}$ has attracted much interest for advancing functional material in recent years.[17−19] Piriouet et al.[20] and Thimet et al.[21] have studied luminescent properties of magnesium cordierite ($Mg_2Al_4Si_5O_{18}$) doped with Eu^{3+} ion prepared by sol−gel and found the $Mg_2Al_4Si_5O_{18}$ has potential

Received: May 6, 2014
Published: October 17, 2014

   dx.doi.org/10.1021/ic501057r | *Inorg. Chem.* 2014, 53, 11396−11403

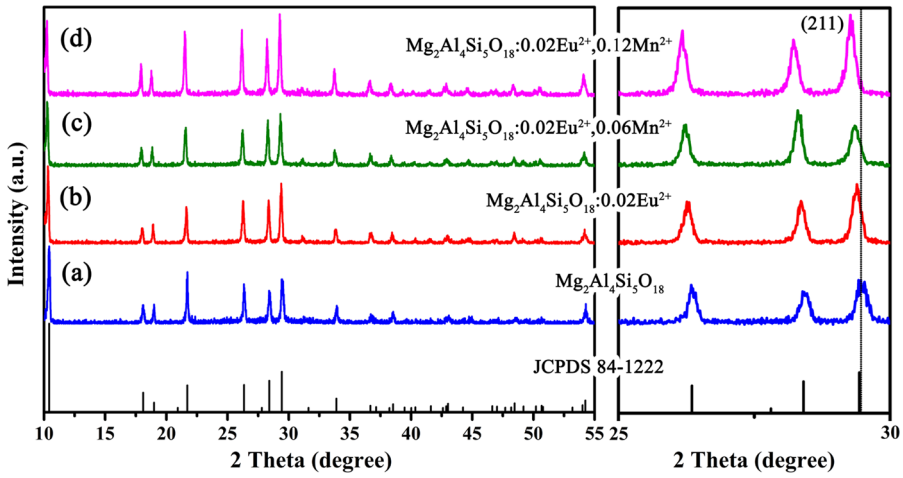

Figure 1. XRD patterns of $Mg_2Al_4Si_5O_{18}$ host, $Mg_2Al_4Si_5O_{18}$: $0.02Eu^{2+}$, xMn^{2+} (x = 0, 0.06, and 0.12), and the standard pattern (JCPDF84−1222) of $Mg_2Al_4Si_5O_{18}$.

application for *w*-LED. In this study, Eu^{2+}- and Mn^{2+}-coactivated $Mg_2Al_4Si_5O_{18}$ phosphors were synthesized by high-temperature solid-state reaction, and their luminescence properties were investigated as a function of activator and coactivator concentrations. Additionally, the energy-transfer mechanism was verified by experimental results of the luminescence spectra, decay curve of the phosphors, and energy-transfer efficiency from Eu^{2+} to Mn^{2+}. The critical distance (Rc) between Eu^{2+} and Mn^{2+} ions was also calculated for the occurrence of energy transfer. All above results indicated that via appropriately adjusting the relative doping concentration ratio of Eu^{2+}/Mn^{2+}, the $Mg_2Al_4Si_5O_{18}$: Eu^{2+}, Mn^{2+} phosphor can emit white light under n-UV light excitation.

2. EXPERIMENTAL DETAILS

2.1. Materials and Syntheses. The $Mg_2Al_4Si_5O_{18}$: Eu^{2+}, Mn^{2+} phosphors were synthesized by traditional high-temperature solid-state reaction. Stoichiometric amounts of MgO (analytical reagent (A. R.)), Al_2O_3 (A. R.), H_2SiO_3 (A. R.), Eu_2O_3 (A. R.), $MnCO_3$, La_2O_3 (A. R.) (An excess of 8 wt% of La_2O_3 was added as flux) were thoroughly mixed via grinding in an agate mortar. The powder mixtures were put into alumina crucible and sintered at 1300 °C for 6 h in a reducing atmosphere (10% H_2 + 90% N_2).

2.2. Characterization Method. The structures of the final products were identified via powder X-ray diffraction on a D8 Advance diffractometer (Germany) with graphite-monochromatized Cu Kα radiation (λ = 0.154 06 nm). The photoluminescence emission (PL) and photoluminescence excitation (PLE) spectra were measured by a Hitachi F-4600 fluorescence spectrophotometer (Japan) equipped with a 150 W Xe lamp as the excitation source. The temperature-dependent luminescence properties were measured using the same spectrophotometer which was assembled with a computer-controlled electric furnace and a self-made heating attachment. Diffuse reflection spectra were performed via a Shimadzu UV-3600 UV−vis−NIR spectrophotometer attached with an integral sphere. The luminescence decay curves were measured from a spectrofluorometer (HORIBA, JOBIN YVON FL3-21) using a tunable pulse laser radiation (nano-LED) as the excitation.

3. RESULTS AND DISCUSSIONS

3.1. Phase Analysis. Figure 1 displays the XRD patterns of $Mg_2Al_4Si_5O_{18}$: $0.02Eu^{2+}$, xMn^{2+} (x = 0, 0.06, and 0.12), and the standard pattern (JCPDF84−1222) of $Mg_2Al_4Si_5O_{18}$, which has a hexagonal structure (space group: *P6/mcc*). The corresponding lattice constants of the standard pattern are as follows: $a = b$ = 9.794 Å, c = 9.339 Å, V = 775.70 Å^3 and Z = 2.[22] All the diffraction peaks of these samples can be matched well with JCPDS Card No. 84−1222, and no impurity was found. As the amount of Eu^{2+} and Mn^{2+} ions was increased in the host lattice, the main diffraction peak of (211) shifted to lower diffraction angles from 29.42° for $Mg_2Al_4Si_5O_{18}$ host to 29.27° for $Mg_2Al_4Si_5O_{18}$: $0.02Eu^{2+}$, $0.12Mn^{2+}$. Meanwhile, the calculated lattice parameters of $Mg_2Al_4Si_5O_{18}$:$0.02Eu^{2+}$, xMn^{2+} phosphors are given in Table 1. As shown in Table 1, the unit cell volume

Table 1. Crystallographic Data and Structure Parameters of $Mg_2Al_4Si_5O_{18}$ Host and $Mg_2Al_4Si_5O_{18}$:$0.02Eu^{2+}$, xMn^{2+} (x = 0, 0.06, and 0.12)

	a (Å) = b (Å)	c (Å)	V (Å^3)
$Mg_2Al_4Si_5O_{18}$	9.7928	9.3414	775.82
$Mg_2Al_4Si_5O_{18}$: $0.02Eu^{2+}$	9.8023	9.3523	778.22
$Mg_2Al_4Si_5O_{18}$: $0.02Eu^{2+}$, $0.06Mn^{2+}$	9.8142	9.3615	780.88
$Mg_2Al_4Si_5O_{18}$: $0.02Eu^{2+}$, $0.12Mn^{2+}$	9.8282	9.3639	783.32

becomes slightly larger with increasing Eu^{2+} and Mn^{2+} doping concentration. These changes of the XRD patterns reveal that the lattice distorted by substitution the ions which are comparatively small radius in $Mg_2Al_4Si_5O_{18}$ host lattice with Eu^{2+} and Mn^{2+} ions, and they also indicate the solid solution of $(Mg_{1-x-y}Eu_xMn_y)_2Al_4Si_5O_{18}$ have formed in crystal structure. Furthermore, the concentrations of Eu^{2+} and Mn^{2+} ions were measured via inductively coupled plasma−atomic emission spectroscopy (ICP-AES) experiment as shown in Table 2. Quantitative analysis of the obtained phosphor by ICP-AES shows that the doping concentrations of Eu^{2+} ions are almost same for the three samples [$(Mg_{1-0.01-x}Eu_{0.01}Mn_x)_2Al_4Si_5O_{18}$ (x = 0.02, 0.06, 0.10)] and Mn^{2+} concentrations can be determined to be 0.015 11, 0.056 80, and 0.095 29, respectively,

Table 2. Results of ICP-AES Analysis of $Mg_2Al_4Si_5O_{18}$:$0.02Eu^{2+}$, xMn^{2+} (x = 0.02, 0.06, and 0.10)

	Mg	Eu	Mn
stoichiometric	1.98 − x	0.02	x
x = 0.02	1.9652	0.0197	0.0151
x = 0.06	1.9239	0.0193	0.0568
x = 0.10	1.8848	0.0199	0.0953

dx.doi.org/10.1021/ic501057r | *Inorg. Chem.* 2014, 53, 11396−11403

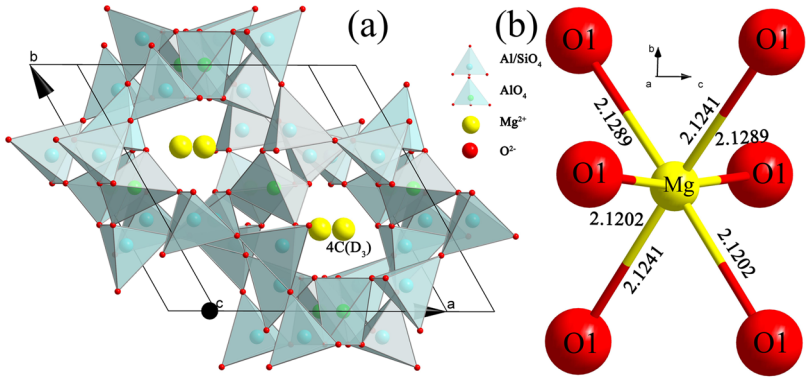

Figure 2. Crystal structures of $Mg_2Al_4Si_5O_{18}$ (a), the coordination environment of the Mg (b).

showing the same increasing tendency with the increasing doping of precursor.

The crystal structure of $Mg_2Al_4Si_5O_{18}$, which is composed of six tetrahedral units $[Si/AlO_4]$ and connected by the $[MgO_6]$ octahedra and $[AlO_4]$ tetrahedra[23], is illustrated in Figure 2. The Mg^{2+} site (4C) is 6-fold coordinated with D_3 point symmetry. Furthermore, the Al and Si atoms are tetrahedrally coordinated via four O atoms. From the consideration of the ionic charge and the radius, Eu^{2+} (r = 1.17 Å when coordinate number (CN) = 6) and Mn^{2+} (r = 0.83 Å when CN = 6) should substitute the position of Mg^{2+} sites (r = 0. 72 Å when CN = 6) because both the Al^{3+} (r = 0.39 Å), and the Si^{4+} (r = 0. 26 Å) sites are too small to accommodate the Eu^{2+} and Mn^{2+} ions.[20,21] Thus, the Eu^{2+} and Mn^{2+} ions should enter into the Mg^{2+} ions site in the $Mg_2Al_4Si_5O_{18}$ lattice.

3.2. Photoluminescence Properties of $Mg_2Al_4Si_5O_{18}$: Eu^{2+}, Mn^{2+}. To further investigate the chemical states of europium and manganese, XPS technique was used to verify the valence of europium and manganese. Photoelectron survey spectra of the $Mg_2Al_4Si_5O_{18}$: $0.02Eu^{2+}$, $0.02Mn^{2+}$ sample is plotted in Figure 3, revealing photoelectron peaks corresponding to Mg 1s, Mg 2s, Eu 3d, Mn 2p, Al 2p, Si 2s, Si 2p, and O 1s emissions. Figure 4a,b exhibits the high-resolution XPS spectra at the Eu 3d and Mn 2P position, respectively. As Figure 3a shows, there are two peaks at 1126.36 and 1133.99 eV, and the shapes as well as binding energies of the Eu 3d signals in $Mg_2Al_4Si_5O_{18}$: Eu^{2+}, Mn^{2+} agree well with the signals of Eu^{2+} $3d_{5/2}$ and Eu^{3+} $3d_{5/2}$, respectively.[24] The existence of peak near 1133.99 eV ascribed to Eu^{3+} $3d_{5/2}$ is because the XPS technique can only measure the elements content in the surface of

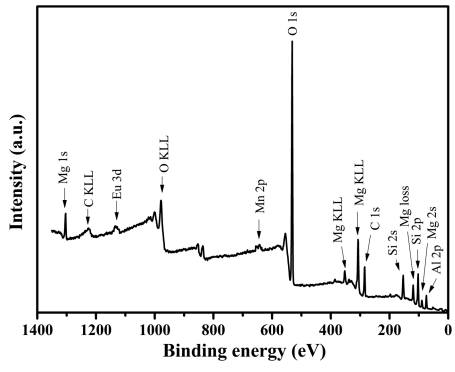

Figure 3. XPS survey spectrum of $Mg_2Al_4Si_5O_{18}$: $0.02Eu^{2+}$, $0.02Mn^{2+}$ phosphors.

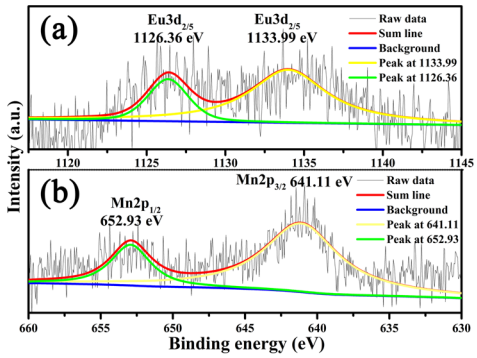

Figure 4. High-resolution XPS spectra at Eu 3d and Mn 2p position of $Mg_2Al_4Si_5O_{18}$: $0.02Eu^{2+}$, $0.02Mn^{2+}$ phosphors.

samples where Eu^{2+} is easily to be oxidized under an ambient atmosphere. As shown in Figure 4b, two broad peaks maximum at 641.11 and 652.93 eV are detected, and they match well with the signals of the binding energy of Mn $2p_{3/2}$ and Mn $2p_{1/2}$, respectiviely. Because the binding energy of Mn 2p is close to the average value of 641.12 eV for Mn^{2+} ions,[25] it is rational to regard as Mn being oxidation states of 2+ in $Mg_2Al_4Si_5O_{18}$: Eu, Mn.

Figure 5a shows the PLE and PL spectra of $Mg_2Al_4Si_5O_{18}$: $0.02Eu^{2+}$. The PLE spectrum exhibits broad excitation from 225 to 425 nm, which originate from 4f−5d transition of Eu^{2+} ions. The wide range of absorption indicates the phosphor can be efficient excited via the n-UV LEDs chip (350−420 nm). Upon 365 nm excitation, the phosphor presents similar blue emission band peaked at 469 nm, which is attributed to $4f^65d-4f^7$ transitions of Eu^{2+}.[26] As the Mn^{2+} singly doped $Mg_2Al_4Si_5O_{18}$ host, its PLE and PL spectra are shown in Figure 5b. The excitation spectrum consists of several bands peaking at 320, 340, 413, and 460 nm, corresponding to the transitions of Mn^{2+} ion from ground level $^6A_1(^6S)$ to $^4E(D)$, $^4T_2(^4D)$, $[^4A_1(^4G)$, $^4E(^4G)]$, and $^4T_1(^4G)$ levels, respectively. The broad emission band from 525 to 750 nm peaked at 600 nm assigned to the spin-forbidden $^4T_1(4G) \rightarrow {}^6A_1(6S)$ transition of $3d^5$ level of Mn^{2+} ions.[27,28] As seen in Figure 5a,b, the comparison of the PL spectrum of $Mg_2Al_4Si_5O_{18}$: Eu^{2+} phosphor and PLE spectrum of $Mg_2Al_4Si_5O_{18}$: Mn^{2+} phosphor show a significant spectral overlap between the Mn^{2+} excitation transitions of $^6A_1(^6S) \rightarrow {}^4T_1(^4G)$, $[^4A_1(^4G)$, $^4E(^4G)]$ and the emission spectrum of Eu^{2+} peaked at 469 nm. Thus, the effective resonance-type energy transfer between the sensitizer Eu^{2+} ions and the activator Mn^{2+} ions is expected. Figure 5c gives the excitation [photoluminescence excitation (PLE); λ_{em} = 469 and

dx.doi.org/10.1021/ic501057r | Inorg. Chem. 2014, 53, 11396−11403

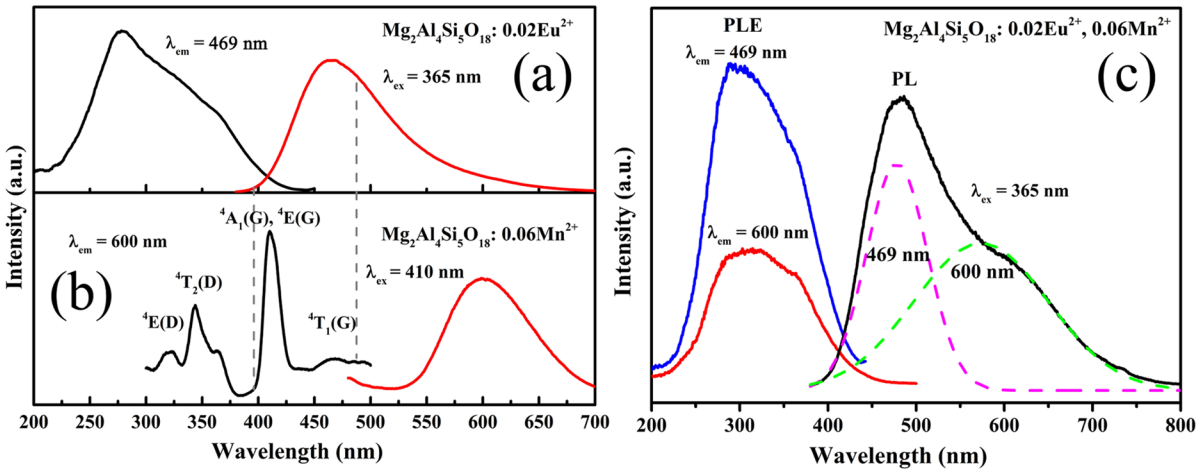

Figure 5. Excitation (left) and emission (right) spectra of $Mg_2Al_4Si_5O_{18}$: $0.02Eu^{2+}$ and $Mg_2Al_4Si_5O_{18}$: $0.06Mn^{2+}$ (b); PLE and PL spectra of $Mg_2Al_4Si_5O_{18}$: $0.02Eu^{2+}$, $0.06Mn^{2+}$ (a). The corresponding monitoring wavelengths are also given in the figure.

600 nm] and emission [photoluminescence (PL); λ_{ex} = 365 nm] spectra of $Mg_2Al_4Si_5O_{18}$: $0.02Eu^{2+}$, $0.06Mn^{2+}$. Using Gaussian deconvolution, the PL spectrum of the $Mg_2Al_4Si_5O_{18}$: $0.02Eu^{2+}$, $0.06Mn^{2+}$ phosphor can be disassembled into two bands peaked at ∼469 and 600 nm, which are consistent with Figure 5a,b, respectively. The PLE of $Mg_2Al_4Si_5O_{18}$: $0.02Eu^{2+}$, $0.06Mn^{2+}$ detected at 469 nm (Eu^{2+} emission) is similar to that detected at 600 nm (Mn^{2+} emission) in addition to the difference of the relative intensity, which is a typical sign of resonance energy transfer. Under 365 nm excitation, the $^4T_1(4G) \rightarrow {}^6A_1(6S)$ transition of Mn^{2+} ions is directly pump. Meanwhile, the $^4T_1(4G) \rightarrow {}^6A_1(6S)$ transition of Mn^{2+} is increased by resonance-type energy transfer from Eu^{2+} to Mn^{2+}. However, the direct absorption and emission of Mn^{2+} are weak owing to the forbidden d−d transitions of Mn^{2+}. Therefore, the main energy gained of Mn^{2+} ion in $Mg_2Al_4Si_5O_{18}$: Eu^{2+}, Mn^{2+} comes from the energy transfer of Eu^{2+} to Mn^{2+}.

To further study the energy absorption of the $Mg_2Al_4Si_5O_{18}$ phosphors, the reflectance spectra of $Mg_2Al_4Si_5O_{18}$, $Mg_2Al_4Si_5O_{18}$: $0.02Eu^{2+}$ and $Mg_2Al_4Si_5O_{18}$: $0.02Eu^{2+}$, $0.06Mn^{2+}$ phosphors are shown in Figure 6. Apparently, The $Mg_2Al_4Si_5O_{18}$ host material exhibits an absorption band from 200 to 300 nm, which is assigned to the host absorption. As Eu^{2+} ions are doped into the host, an obvious absorption from 250 to 400 nm assigned to the $4f^7-4f^65d^1$ absorption of the Eu^{2+} ions is observed. Moreover, with the introduction of Mn^{2+} ions in the former $Mg_2Al_4Si_5O_{18}$: $0.02Eu^{2+}$, the absorption band of $Mg_2Al_4Si_5O_{18}$: $0.02Eu^{2+}$, $0.06Mn^{2+}$ is similar as that of $Mg_2Al_4Si_5O_{18}$: $0.02Eu^{2+}$. Above results are consistent with the PLE spectra (Figure 5) and demonstrate that the broad and strong absorption range of $Mg_2Al_4Si_5O_{18}$: Eu^{2+}, Mn^{2+} are matching well with near UV chips.

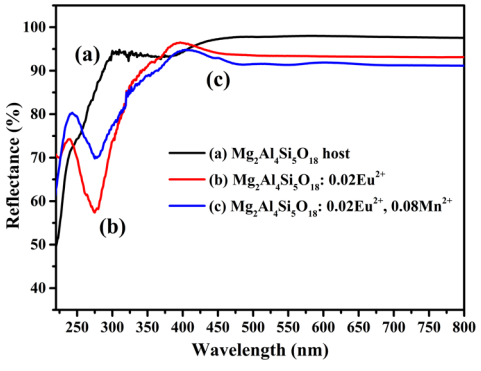

Figure 6. Diffuse reflectance spectra of $Mg_2Al_4Si_5O_{18}$ host (a), $Mg_2Al_4Si_5O_{18}$: $0.02Eu^{2+}$ (b), and $Mg_2Al_4Si_5O_{18}$: $0.02Eu^{2+}$, $0.06Mn^{2+}$ (c) phosphors.

The PL spectra by excitation at 365 nm for Eu^{2+} and Mn^{2+} -coactivated $Mg_2Al_4Si_5O_{18}$: $0.02Eu^{2+}$, xMn^{2+} phosphors with different dopant contents x of 0, 0.01, 0.02, 0.03, 0.04, 0.05, 0.06, 0.08, 0.10, and 0.12 are presented in Figure 7. It revealed

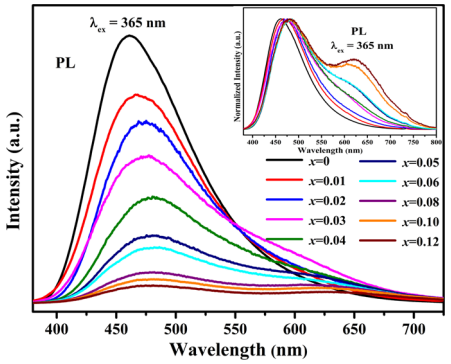

Figure 7. PL spectra for $Mg_2Al_4Si_5O_{18}$: $0.02Eu^{2+}$, xMn^{2+} (x = 0−0.12) phosphors. (inset) The normalized PL spectra for $Mg_2Al_4Si_5O_{18}$: $0.02Eu^{2+}$, xMn^{2+} (x = 0−0.12) phosphors.

that the intensity of Eu^{2+} sensitizer (or energy donor) decrease obviously as the concentrations of Mn^{2+} increased gradually, reflecting the result of energy transfer from Eu^{2+} to Mn^{2+}. As the inset of Figure 7 presents, with the content of Mn^{2+} increases gradually, a red-shift of the peak wavelength of Eu^{2+} is observed which was due to the changes of the crystal field strength circumambient the activators.[29,30] The crystal field strength is inversely proportional to the distance from the coordinate groups to the central positive ion. The substitutions of Eu^{2+} and Mn^{2+} for Mg^{2+}, whose ionic radius shows large difference, will result in the expansion of the lattice and change the covalence and bond length. Eventually, the positions of splitting components of the Eu^{2+} 5*d* band would be reduced by above variation and bring about the red-shift.

Figure 8 demonstrates the variation of the emission intensities of the 4f−5d transition of Eu^{2+} at 469 nm and

dx.doi.org/10.1021/ic501057r | Inorg. Chem. 2014, 53, 11396−11403

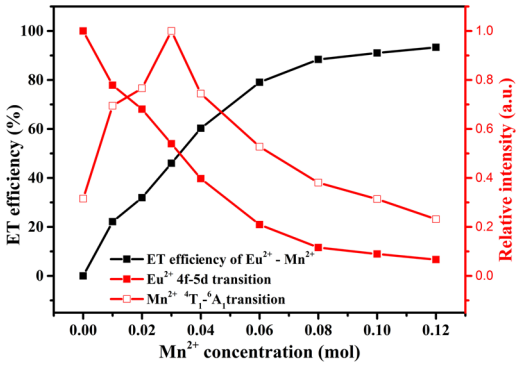

Figure 8. Dependence of the Eu^{2+} emission, Mn^{2+} emission, and energy-transfer efficiency of Eu^{2+}–Mn^{2+} on Mn^{2+} doping concentration for $Mg_2Al_4Si_5O_{18}$: 0.02Eu^{2+}, $x$$Mn^{2+}$ (x = 0–0.12) phosphors.

$^4T_1$–$^6A_1$ transition of Mn^{2+} at 600 nm as a function of Mn^{2+} concentrations, respectively, and the energy-transfer efficiency of Eu^{2+} → Mn^{2+} in $Mg_2Al_4Si_5O_{18}$: 0.02Eu^{2+}, $x$$Mn^{2+}$ phosphor. Generally, the energy-transfer efficiency can be expressed as follows:[31]

$$\eta_T = 1 - \frac{I_x}{I_0} \quad (1)$$

where η_T is the energy transfer efficiency, I_0 and I_x are the luminescence intensity of the sensitizer (Eu^{2+}) in the absence and presence of the activator (Mn^{2+}), respectively. Obviously, the Eu^{2+} relative emission intensities decrease with the increasing concentration of Mn^{2+} dramatically due to the enhancement of energy transfer from the Eu^{2+} to Mn^{2+}, whereas the relative emission intensities of Mn^{2+} ions increase initially and attains the saturation at x = 0.03, and then decreased when x exceeded 0.03, which is primarily due to the Mn^{2+}–Mn^{2+} internal concentration quenching.[16,31,32] Consequently, the relative ratio of the emission intensities of Eu^{2+} and Mn^{2+} could be tuned via properly adjusting the Mn^{2+} concentration.

The room-temperature decay curves for the $Mg_2Al_4Si_5O_{18}$: 0.02Eu^{2+}, $x$$Mn^{2+}$ (x = 0–0.12) phosphors monitored at 469 nm for Eu^{2+} emission and 600 nm for Mn^{2+} emission were measured and are represented in Figure 9a,b, respectively. All the decay curves monitored at (a) 469 nm for Eu^{2+} emission can be well-fitted via the double-exponential equation:[33]

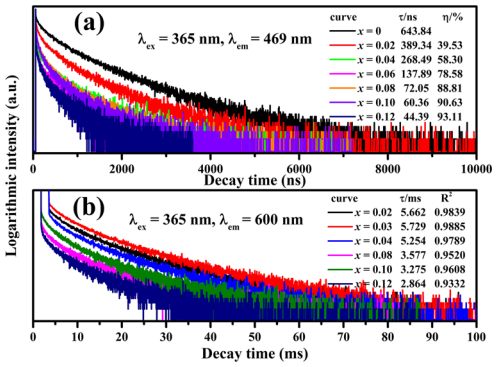

Figure 9. Decay lifetime tests of $Mg_2Al_4Si_5O_{18}$: 0.02Eu^{2+}, $x$$Mn^{2+}$ (x = 0–0.12) detected at (a) 469 nm for Eu^{2+} emission and (b) 600 nm for Mn^{2+} emission.

$$I(t) = A_1\exp(-t/\tau_1) + A_2(-t/\tau_2) \quad (2)$$

where I is the luminescence intensity; A_1 and A_2 are constants; t is time; and τ_1 and τ_2 are the lifetimes for the exponential components. Further, the average lifetime constant (τ^*) can be estimated as

$$\tau^* = (A_1\tau_1^2 + A_2\tau_2^2)/(A_1\tau_1 + A_2\tau_2) \quad (3)$$

According to eqs 2 and 3, the average lifetimes (τ) can be reckoned to 643.84, 389.34, 268.49, 137.89, 72.05, 60.36, 44.39 ns for $Mg_2Al_4Si_5O_{18}$: 0.02Eu^{2+}, $x$$Mn^{2+}$ with x = 0, 0.02, 0.04, 0.06, 0.08, 0.10, and 0.12, respectively. It clearly shows that the lifetime of Eu^{2+} ions monotonically decreases with the increasing amount of Mn^{2+} ions. The energy-transfer efficiency can be estimated via the following expression:[27,34]

$$\eta_T = 1 - \frac{\tau_x}{\tau_0} \quad (4)$$

where τ_0 and τ_x are the lifetimes of the sensitizer with and without the activator, and η_T is the calculation of energy-transfer efficiency. The energy-transfer efficiency from the sensitizer Eu^{2+} to the activator Mn^{2+}, which estimated via above equation, is given in the inset of Figure 9a. With increasing Mn^{2+} dopant content, the η_T increases and in good agreement with that obtained above in Figure 8. As Figure 9b shows, the decay curves of $Mg_2Al_4Si_5O_{18}$: 0.02Eu^{2+}, $x$$Mn^{2+}$ (x = 0–0.12) phosphors monitored at 469 nm are gradually got less linear with increasing Mn^{2+} concentration, which is a typical sign of energy transfer, and eventually causes concentration quenching.[30] The corresponding decay times were fitted well by single-exponential function ($I(t)$ = A $\exp(-t/\tau)$), and the lifetimes detected at 600 nm can be calculated to 5.729, 5.662, 4.254, 3.577, 3.275, and 2.864 ms with x = 0.02, 0.03, 0.06, 0.08, 0.10, and 0.12, respectively. The measured lifetimes of $Mn^{2+4}T_1(4G)$ → $^6A_1(6S)$ emission increase with the increasing concentration of Mn^{2+}, and then decline sharply at maximum value of x = 0.03, which also confirms the energy transfer exist between Eu^{2+}–Mn^{2+} and Mn^{2+}–Mn^{2+} and causes concentration quenching.[35]

According to the concentration quenching method, the critical distance R_c was estimated for the energy transfer from Eu^{2+} to Mn^{2+}. On various occasions, concentration quenching is due to energy transfer from one activator to another until an energy sink in the lattice is reached.[36] The average distance R_{Eu-Mn} between Eu^{2+} and Mn^{2+} can be expressed via the relation given by Blasse[37]

$$R_{Eu-Mn} = 2\left[\frac{3V}{4\pi x_c N}\right]^{1/3} \quad (5)$$

where N is the number of Z ions in the unit cell, V is the volume of the unit cell and x is the total concentration of Eu^{2+} and Mn^{2+}. For $Mg_2Al_4Si_5O_{18}$ host, N = 2 and V = 775.70 Å^3.[22] If the critical concentration x_c, where the luminescence intensity of Eu^{2+} reduces to half of that for the sample without Mn^{2+}, is used in the above equation, R_c can be obtained. The critical concentration $x_c \approx 0.02 + 0.036 = 0.056$. Consequently, the critical distance (R_c) of energy transfer can be reckoned to 23.65 Å.

To further research the energy transfer mechanism from Eu^{2+} to Mn^{2+} ions, we can obtain the following relation for exchange and multipolar interactions by Dexter's energy transfer formula:[38–40]

dx.doi.org/10.1021/ic501057r | Inorg. Chem. 2014, 53, 11396–11403

$$\ln\left(\frac{\eta_0}{\eta}\right) \propto \mathrm{Cand}\frac{\eta_0}{\eta} \propto C^{n/3} \quad (6)$$

where η_0 and η are the luminescence quantum efficiency of Eu^{2+} in the absence and presence of Mn^{2+}, respectively; C is the total dopant concentration of Eu^{2+} and Mn^{2+}. The relationship of $\ln(\eta_{S0}/\eta_S) \propto C$ corresponds to the exchange interaction, and n = 6, 8, and 10 corresponding to dipole−dipole, dipole−quadrupole, and quadrupole−quadrupole interactions, respectively. The value η_0/η can be approximately estimated by the following relation[36,38]

$$\ln\left(\frac{I_0}{I}\right) \propto \mathrm{Cand}\frac{I_{S0}}{I_S} \propto C^{n/3} \quad (7)$$

in which I_{S0} and I_S are the luminescence intensity of Eu^{2+} with and without Mn^{2+} present. The relationships between $\ln(I_{S0}/I_S)$ and $C^{n/3}$ well as I_{S0}/I_S and $C^{n/3}$ are illustrated in Figure 10a-d,

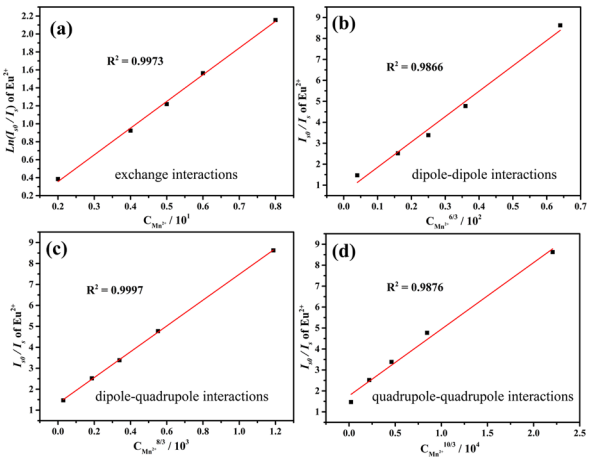

Figure 10. Dependence of $\ln(I_{S0}/I_S)$ of Eu^{2+} on C_{Mn2+} (a) and I_{s0}/I_s of Eu^{2+} on $C_{Mn2+}{}^{6/3}$ (b), $C_{Mn2+}{}^{8/3}$ (c), $C_{Mn2+}{}^{10/3}$ (d).

and The R^2 value for Figure 10c of the linear fit was estimated to be 0.9997, which indicates that the curve is most similar to the linear relation when n = 8, suggesting that the energy transfer of $Eu^{2+} \rightarrow Mn^{2+}$ follows a dipole−quadrupole mechanism in $Mg_2Al_4Si_5O_{18}$: Eu^{2+}, Mn^{2+} phosphor. Hence, the critical distance (R_c) of energy transfer from Eu^{2+} to Mn^{2+} can be calculated by the following simplified equation:[5]

$$R_C{}^8 = 0.63 \times 10^{28}\frac{f_q\lambda_S{}^2 Q_A}{f_d E_S{}^4}\int F_S(E)F_A(E)\mathrm{d}E \quad (8)$$

here Q_A is the absorption coefficient of Mn^{2+}, which is equal to 4.8×10^{-16} f_d given by Dexter;[41] $f_d = 10^{-7}$ and $f_q = 10^{-10}$ are the oscillator strengths of the dipole and quadrupole electrical absorption transitions for Mn^{2+}, respectively; λ_S (in Å) and E (in eV) represent the wavelength position of Eu^{2+} emission and the energy involved in the transfer, respectively; $\int F_S(E)F_A(E)\mathrm{d}E$ means the spectral overlap between the normalized shapes of Eu^{2+} emission $F_S(E)$ and Mn^{2+} excitation $F_A(E)$. Therefore, the R_c for Eu → Mn energy transfer in $Mg_2Al_4Si_5O_{18}$: Eu, Mn was estimated to be 22.89 Å, which is in good accord with the result reckoning by concentration quenching method.

3.2. Thermal Quenching Property and CIE of $Mg_2Al_4Si_5O_{18}$: Eu^{2+}, Mn^{2+}. As we know, the thermal quenching property of phosphor is one of the important properties in the white LED application, which is considerable influence chromaticity and brightness of white light output. Therefore, the temperature dependence of the luminescence for $Mg_2Al_4Si_5O_{18}$:0.02Eu^{2+} and $Mg_2Al_4Si_5O_{18}$:0.02Eu^{2+}, 0.04Mn^{2+} under 365 nm excitation is shown in Figure 11.

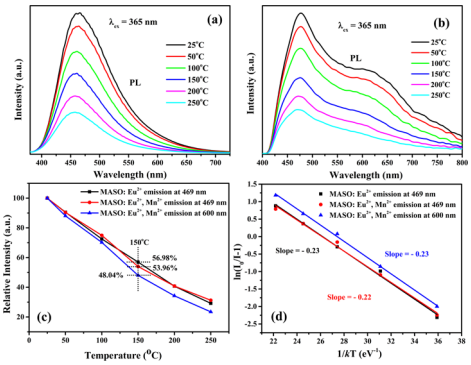

Figure 11. Temperature-dependent PL spectra of the $Mg_2Al_4Si_5O_{18}$:0.02Eu^{2+} (a) and $Mg_2Al_4Si_5O_{18}$:0.02Eu^{2+}, 0.04Mn^{2+} (b) phosphors, and the emission intensity versus temperature (c). The plot of ln (I_0/I) vs $1/T$ of the $Mg_2Al_4Si_5O_{18}$:0.02Eu^{2+} and $Mg_2Al_4Si_5O_{18}$:0.02Eu^{2+}, 0.04Mn^{2+} phosphors (d).

Since the LED package would generate heat during the LED operation, the phosphors of the white LEDs are required to maintain their conversion efficiency up to 150 °C.[42] As shown in Figure 11a, the PL intensities of $Mg_2Al_4Si_5O_{18}$:0.02Eu^{2+} reduce to 56.98% of the initial intensities at room temperature and then further decrease to 29.19% at 250 °C. The temperature dependence of the emission for $Mg_2Al_4Si_5O_{18}$:0.02Eu^{2+}, 0.04Mn^{2+} is illustrated in Figure 11b. The intensities of the characteristic peaks of Eu^{2+} and Mn^{2+} are declined to 53.96% and 48.04% of the value before heating up, respectively, with the temperature increasing to 150 °C, which is approximated that of the $Mg_2Al_4Si_5O_{18}$:0.02Eu^{2+} phosphor. The emission intensity decreased with temperature increment is attributed to the interaction of electron−phonon in both the ground state and excited state of luminescence center, and this nonradiative transition probability dependent on temperature, leading to the decrease in emission intensity.[43] To further research temperature dependence of luminescence, the activation energy was estimated via the Arrhenius equation:[44]

$$I(T) \approx \frac{I_0}{1 + c\exp\left(\frac{-\Delta E}{kT}\right)} \quad (9)$$

in which I_0 and $I(T)$ are the initial luminescence intensity of the sample at room temperature and the testing temperature, respectively, ΔE is the activation energy for the thermal quenching, c is a constant, and k is the Boltzman's constant (8.62×10^{-5} eV). The activation energy is energy level difference between the lowest energy level of relaxed excited level and the host lattice conduction band level.[45] Hence, in the same or similar crystal structure, the higher the activation energy ΔE is, the better the thermal stability is.[46] Figure 11d illustrates the activation energy of the $Mg_2Al_4Si_5O_{18}$:0.02Eu^{2+} and $Mg_2Al_4Si_5O_{18}$:0.02Eu^{2+}, 0.04Mn^{2+} phosphors. The activation energies (ΔE) was estimated as 0.23 for $Mg_2Al_4Si_5O_{18}$:0.02Eu^{2+} via plotting $\ln[(I_0/I) - 1]$ against $1/kT$, where a straight slope equals $-\Delta E$, and the activation

dx.doi.org/10.1021/ic501057r | Inorg. Chem. 2014, 53, 11396−11403

energies (ΔE) of $Mg_2Al_4Si_5O_{18}$:0.02Eu^{2+}, 0.04Mn^{2+} emission at 469 and 600 nm were calculated as 0.22 and 0.23, respectively.

The CIE chromaticity coordinates of the single-phased emission-tunable $Mg_2Al_4Si_5O_{18}$:0.02Eu, *x*Mn phosphors upon 365 nm excitation are portrayed in Figure 12. It can be seen

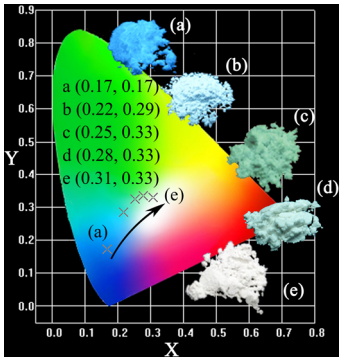

Figure 12. Representation of the CIE chromaticity coordinates for $Mg_2Al_4Si_5O_{18}$:0.02Eu, *x*Mn (a) $x = 0$; (b) $x = 0.02$; (c) $x = 0.04$; (d) $x = 0.08$; (e) $x = 0.10$) phosphors under 365 nm excitation and the selected samples digital images excited at 365 nm in UV box.

that the CIE chromaticity coordinates move from blue (0.17, 0.17) to bluish green (0.22, 0.29), and finally to white (0.31, 0.33) as the amount of Mn^{2+} varies from 0.00 to 0.12. The images of the emitting phosphors are given in the inset and the as-observed emitting color is very obvious. Color rendering index (CRI) and correlated color temperature (CCT) is a qualitative measure of the ability to display the colors of an irradiated object in a natural way,[47] and the CRI and CCT values of the samples are demonstrated in Table 3. It is noteworthy that white light with a desired CRI can be achieved as the doped content of Mn^{2+} is controlled to 0.10 mol.

Table 3. CRI and CCT Values of $Mg_2Al_4Si_5O_{18}$:0.02Eu, *x*Mn Samples

sample	CIE(x, y)	CRI	CCT [K]
$Mg_2Al_4Si_5O_{18}$:0.02Eu, 0.10Mn	(0.309, 0.336)	89.29	6831
$Mg_2Al_4Si_5O_{18}$:0.02Eu, 0.12Mn	(0.307, 0.331)	88.05	7006

To further assess the potential application of $Mg_2Al_4Si_5O_{18}$: Eu^{2+}, Mn^{2+} phosphor for white LEDs, a *w*-LED lamp was fabricated using a 385 nm NUV chip combined with single-phase white-emitting $Mg_2Al_4Si_5O_{18}$: 0.02Eu^{2+}, 0.10Mn^{2+} phosphor.[48] The electroluminescent (EL) spectrum of this *w*-LED lamp driven by 30 mA current is illustrated in Figure 13. The inset exhibits the image of the LED lamp package driven by 30 mA current. The EL spectrum obviously displays three emission bands at 385, 480, and 610 nm, which derive from the 385 nm NUV chip, Eu^{2+} emission, and Mn^{2+} emission, respectively. The *w*-LED lamp produces CIE color coordinates of (0.32, 0.35) with a correlated color temperature of 6277.82 K and color rendering index values of 88.62, suggesting that the composition-optimized $Mg_2Al_4Si_5O_{18}$: 0.02Eu^{2+}, 0.10Mn^{2+} phosphor can be used as a promising white-emitting phosphor for white-light NUV LEDs.

4. CONCLUSION

In conclusion, a series of single-phased and color-tunable $Mg_2Al_4Si_5O_{18}$: Eu^{2+}, Mn^{2+} phosphors have been prepared by

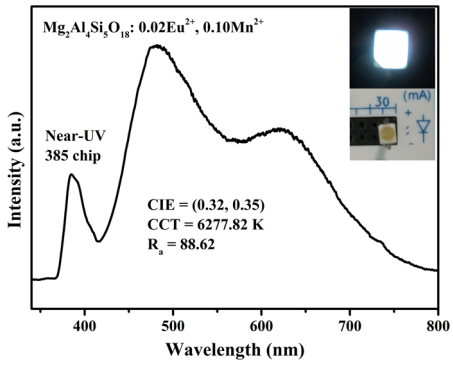

Figure 13. Electroluminescence spectra of *w*-LED lamp fabricated via the combination of a NUV 385 nm chip and white-emitting $Mg_2Al_4Si_5O_{18}$:0.02Eu^{2+}, 0.10Mn^{2+} phosphor. (inset) Digital images of the LED package with and without powder input.

high-temperature solid-state reaction, and their luminescence properties and energy-transfer behavior were investigated in detail. The spectroscopic data indicate that the energy-transfer process from Eu^{2+} to Mn^{2+} occurs in the $Mg_2Al_4Si_5O_{18}$ host. The $Eu^{2+} \rightarrow Mn^{2+}$ energy transfer has been determined to be a resonant type via a dipole−quadrupole mechanism. In addition, the energy-transfer critical distance was reckoned via the concentration-quenching (23.65 Å) and spectral-overlap (22.89 Å) methods, respectively, and the values reckoned by the two methods are in good accord. The emission color can be tuned from blue (0.17, 0.17) to bluish-green (0.22, 0.29) and finally to white (0.31, 0.33) via appropriately tuning the concentration of Mn^{2+}. These results indicate that $Mg_2Al_4Si_5O_{18}$: Eu^{2+}, Mn^{2+} phosphor may have a potential application to serve as a single-composition white-emitting phosphor under UV excitation.

AUTHOR INFORMATION

Corresponding Author

*E-mail: liuyang@cugb.edu.cn.

Notes

The authors declare no competing financial interest.

ACKNOWLEDGMENTS

This project is financially supported by National Natural Science Foundation of China (Grant No. 51472223), the Program for New Century Excellent Talents in University of Ministry of Education of China (Grant No. NCET-12-0951) and the Fundamental Research Funds for the Central Universities (Grant No. 2012067).

REFERENCES

(1) Höppe, H. A. *Angew. Chem., Int. Ed.* **2009**, *48*, 3572−3582.
(2) Lin, C. C.; Liu, R. S. *J. Phys. Chem. Lett.* **2011**, *11*, 1268−1277.
(3) Shang, M. M.; Li, C. X.; Lin. *J. Chem. Soc. Rev.* **2014**, *43*, 1372−1386.
(4) Nakamura, S.;, Fasol, G. *The Blue Laser Diode;* Springer: Berlin, Germany, 1996.
(5) Won, Y. H.; Jang, H. S.; Im, W. B.; Lee, J. S.; Jeon, D. Y. *Appl. Phys. Lett.* **2006**, *89*, 231909−231909−3.
(6) Yang, W. J.; Lou, L. Y.; Chen, T. M.; Wang, N. S. *Chem. Mater.* **2005**, *17*, 3883−3888.
(7) Kwon, K. H.; Im, W. B.; Jang, H. S.; Yoo, H. S.; Jeon, D. Y. *Inorg. Chem.* **2009**, *48*, 11525−11532.
(8) Shi, L.; Huang, Y.; Seo, H. J. *J. Phys. Chem. A* **2010**, *114*, 6927−6934.
(9) Barry, T. L. *J. Electrochem. Soc.* **1970**, *117*, 381−385.

(10) Rubio, J. O.; Murrieta, S. H.; Powell, R. C.; Sibley, W. A. *Phys. Rev. B* **1985**, *31*, 59−67.
(11) Caldino, U. G.; Munoz, A. F.; Rubio, J. O. *J. Phys.: Condens. Matter* **1990**, *2*, 6071−6078.
(12) Caldino, U. G.; Munoz, A. F.; Rubio, J. O. *J. Phys.: Condens. Matter* **1993**, *5*, 2195−2202.
(13) Mendez, A.; Ramos, F. L.; Riceros, H.; Camarillo, E.; Caldino, U. G. *J. Mater. Sci. Lett.* **1999**, *18*, 399−402.
(14) Yang, W. J.; Chen, T. M. *Appl. Phys. Lett.* **2006**, *88*, 101903−101903−3.
(15) Kim, J. S.; Jeon, P. E.; Choi, J. C.; Park, H. L.; Mho, S. I.; Kim, G. C. *Appl. Phys. Lett.* **2004**, *84*, 2931−2933.
(16) Chang, C. K.; Chen, T. M. *Appl. Phys. Lett.* **2007**, *90*, 161901−161901−3.
(17) Ismail, M. G. M. U.; Tsunatori, H.; Nakai, Z. *J. Am. Ceram. Soc.* **1990**, *73*, 537−543.
(18) Kumar, S.; Singh, K. K.; Ramachandrarao, P. *J. Mater. Sci. Lett.* **2000**, *19*, 1263−1265.
(19) Ianoşev, S.; Lazău, I.; Păcurariu, C.; Avramescu, A. *Proces Appl. Ceram.* **2008**, *2*, 39−44.
(20) Piriou, B.; Chen, Y. F.; Vilminot, S. *Eur. J. Solid State Inorg. Chem.* **1998**, *35*, 341−355.
(21) Thim, G. P.; Brito, H. F.; Silva, S. A.; Oliveira, M. A.; Felinto, M. C. *J. Solid State Chem.* **2003**, *171*, 375−381.
(22) Predecki, P.; Haas, J.; Faber, J.; Hitterman, R. L. *J. Am. Ceram. Soc.* **1987**, *3*, 175−182.
(23) Winchell, A. N.; Winchell, H. *Optical Properties of Artificial Minerals;* Academic Press: New York, 1964.
(24) Chae, K. W.; Park, T. R.; Cheon, C. I.; Cho, N. I.; Kim, J. S. *J. Lumin.* **2011**, *131*, 2597−2605.
(25) Ahmad, A. A.; Peter, M. A. S. *Surf. Interface Anal.* **2002**, *33*, 274−282.
(26) Zeng, Q. H.; Zhang, T. Z.; Pei, Z. W. *J. Mater. Sci. Technol.* **1999**, *15*, 281−282.
(27) Paulose, P. I.; Jose, G.; Thomas, V.; Unnikrishnan, N. V.; Warrier, M. K. R. *J. Phys. Chem. Solids* **2003**, *64*, 841−846.
(28) Geng, D. L.; Li, G. G.; Shang, M. M.; Yang, D. M.; Zhang, Y.; Cheng, Z. Y.; Lin, J. *J. Mater. Chem.* **2012**, *22*, 14262−14271.
(29) Zhou, T. L.; Wang, H. R.; Liu, F. S.; Zhang, H.; Liu, Q. L. *J. Electrochem. Soc.* **2011**, *158*, H671−H674.
(30) Xia, Z. G.; Zhou, J.; Mao, Z. Y. *J. Mater. Chem. C* **2013**, *1*, 5917−5924.
(31) Li, G. G.; Geng, D. L.; Shang, M. M.; Peng, C.; Cheng, Z. Y.; Lin, J. *J. Mater. Chem.* **2011**, *21*, 13334−13344.
(32) Biju, P. R.; Jose, G.; Thomas, V.; Nampoori, V. P. N.; Unnikrishnan, N. V. *Opt. Mater.* **2004**, *24*, 671−677.
(33) Huang, C. H.; Chen, T. M. *Inorg. Chem.* **2011**, *50*, 5725−5730.
(34) Xia, Z. G.; Liu, R. S. *J. Phys. Chem. C* **2012**, *116*, 15604−15609.
(35) Henderson, B.; Imbusch, G. F. *Optical Spectroscopy of Inorganic Solids;* Clarendon, Oxford, U.K., 1989.
(36) Dexter, D. L.; Schulman, J. A. *J. Chem. Phys.* **1954**, *22*, 1063−1067.
(37) Blasse, G. *Philips Res. Rep.* **1969**, *24*, 131−144.
(38) Jiao, H.; Liao, F.; Tian, S.; Jing, X. *J. Electrochem. Soc.* **2003**, *150*, H220−H224.
(39) Reisfeld, R.; Lieblich-sofer, N. *J. Solid State Chem.* **1979**, *28*, 391−395.
(40) Jia, Y. C.; Qiao, H.; Zheng, Y. H.; Guo, N.; You, H. P. *Phys. Chem. Chem. Phys.* **2012**, *14*, 3537−3542.
(41) Dexter, D. L. *J. Chem. Phys.* **1953**, *21*, 836.
(42) Xia, Z. G.; Wu, W. W. *Dalton Trans.* **2013**, *42*, 12989−12997.
(43) Mikhailikm, V. B.; Kraus, H.; Wahl, D.; Itoh, M.; Koike, M.; Bailiff, I. K. *Phys. Rev. B* **2004**, *69*, 20510.
(44) Bhushan, S.; Chukichev, M. V. *J. Mater. Sci. Lett.* **1988**, *7*, 319−321.
(45) Dorenbos, P. *J. Phys.: Condens. Matter.* **2005**, *17*, 8103−8111.
(46) Zhao, C. L.; Xia, Z. G.; Yu, S. X. *J. Mater. Chem. C* **2014**, *2*, 6032−6039.
(47) Bulter, K. H. *Fluorescent Lamp Phosphors;* The Pennsylvania State University Press: University Park, PA, 1980.
(48) Liu, W. R.; Huang, C. H.; Yeh, C. W.; Tsai, J. C.; Chiu, Y. C.; Yeh, Y. T.; Liu, R. S. *Inorg. Chem.* **2012**, *51*, 9636−9641.